The Journal of Infectious Diseases

MAJOR ARTICLE

Regular Use of Depot Medroxyprogesterone Acetate Causes Thinning of the Superficial Lining and Apical Distribution of Human Immunodeficiency Virus Target Cells in the Human Ectocervix

Gabriella Edfeldt,[1] Julie Lajoie,[2,3] Maria Röhl,[1] Julius Oyugi,[2,3] Alexandra Åhlberg,[1] Behnaz Khalilzadeh-Binicy,[1] Frideborg Bradley,[1] Matthias Mack,[4] Joshua Kimani,[2,3,5] Kenneth Omollo,[3] Carolina Wählby,[6,7] Keith R. Fowke,[2,3,5,8] Kristina Broliden,[1,a] and Annelie Tjernlund[1,a]

[1]Division of Infectious Diseases, Department of Medicine Solna, Karolinska Institutet, Karolinska University Hospital, Center for Molecular Medicine, Stockholm, Sweden, [2]Department of Medical Microbiology and Infectious Diseases, University of Manitoba, Winnipeg, Canada, [3]Department of Medical Microbiology, University of Nairobi, Nairobi, Kenya, [4]Department of Internal Medicine–Nephrology, University Hospital Regensburg, Regensburg, Germany, [5]Partners for Health and Development in Africa, Nairobi, Kenya, [6]Department of Information Technology, Uppsala University, Uppsala, Sweden, [7]SciLifeLab BioImage Informatics Facility, Uppsala, Sweden, and [8]Department of Community Health Sciences, University of Manitoba, Winnipeg, Canada

Background. The hormonal contraceptive depot medroxyprogesterone acetate (DMPA) may be associated with an increased risk of acquiring human immunodeficiency virus (HIV). We hypothesize that DMPA use influences the ectocervical tissue architecture and HIV target cell localization.

Methods. Quantitative image analysis workflows were developed to assess ectocervical tissue samples collected from DMPA users and control subjects not using hormonal contraception.

Results. Compared to controls, the DMPA group exhibited a significantly thinner apical ectocervical epithelial layer and a higher proportion of $CD4^+CCR5^+$ cells with a more superficial location. This localization corresponded to an area with a nonintact E-cadherin net structure. $CD4^+Langerin^+$ cells were also more superficially located in the DMPA group, although fewer in number compared to the controls. Natural plasma progesterone levels did not correlate with any of these parameters, whereas estradiol levels were positively correlated with E-cadherin expression and a more basal location for HIV target cells of the control group.

Conclusions. DMPA users have a less robust epithelial layer and a more apical distribution of HIV target cells in the human ectocervix, which could confer a higher risk of HIV infection. Our results highlight the importance of assessing intact genital tissue samples to gain insights into HIV susceptibility factors.

Keywords. female genital mucosa; hormonal contraception; DMPA; HIV; in situ staining; digital image analysis; epithelial integrity; HIV target cells; estradiol; progesterone.

Sub-Saharan Africa bears the greatest burden of human immunodeficiency virus (HIV) infection, with approximately 20 million people living with the condition [1]. In Sub-Saharan Africa injectable hormonal contraceptives are a popular choice of birth control, used by millions of women [2]. However, observational epidemiological studies have demonstrated a significant association between the 3-month progestin-containing injectable contraceptive depot medroxyprogesterone acetate (DMPA) and HIV acquisition [3–5]. Because a recent prospective clinical trial could not confirm a higher HIV infection risk associated with DMPA, the relative risk of DMPA remains controversial [6–8].

Proposed mechanisms of action for DMPA have been extensively evaluated in experimental, animal, and clinical studies [9]. Collectively, these studies demonstrate that DMPA is associated with impaired mucosal integrity and altered immune responses [10–17], which could increase susceptibility to HIV infection. Studies assessing women living in resource-poor HIV-endemic settings have been limited to samples of blood, genital secretions, and cervicovaginal mononuclear cells. As such, data from advanced imaging studies of cervicovaginal tissue samples are scarce [18]. For the present study, a customized image analysis workflow

Received 2 June 2020; editorial decision 3 August 2020; accepted 8 August 2020; published online August 11, 2020.

[a]K. B. and A. T. contributed equally to this work.

Presented in part: Annual Meeting of the Scandinavian Society of Immunology, Stockholm, Sweden, October 2017 (Abstract A31355); Annual Scientific Review and Planning Meeting, University of Nairobi STD/AIDS Collaborative Centre, Nairobi, Kenya, January 2018; and HIV Research for Prevention (HIVR4P) Conference, Madrid, Spain, October 2018 (Abstract P18.19).

Correspondence: Gabriella Edfeldt, PhD, Department of Medicine Solna, Division of Infectious Diseases, Karolinska Institutet, Karolinska University Hospital, Center for Molecular Medicine, 171 64 Stockholm, Sweden (gabriella.edfeldt@ki.se).

The Journal of Infectious Diseases® 2022;225:1151–61

DOI: 10.1093/infdis/jiaa514

was developed to investigate the effect of DMPA usage on ectocervical tissue samples from a cohort of women in Kenya compared with control subjects. With this approach, we were able to obtain data regarding changes in immune cells and tissue structure induced by DMPA usage, as well as its potential impact on HIV susceptibility.

MATERIALS AND METHODS

Study Subjects and Hormone Measurements

This substudy involved women from the Pumwani Sex Worker Cohort in Kenya who had reported sex work for 3 years or less. Subjects were selected from a larger clinical protocol [19, 20] based on DMPA use or no use of hormonal contraceptives. All study subjects answered demographic and behavioral questionnaires, and were sampled at 2 time points 2 weeks apart. Measures such as text messages, on-site prostate-specific antigen detection, and comprehensive informed consent encouraged participants to refrain from vaginal intercourse during the biopsy healing period [20]. To be included in this study, subjects had to be 18–50 years of age, not have started menopause, and have tested negative for HIV, *Neisseria gonorrhoeae*, *Chlamydia trachomatis*, and syphilis infections. Moreover, women in the DMPA group had to have taken DMPA for at least 6 months and were targeted for enrollment within a 2- to 6-week window since their last injection, and women in the control group had to have a regular menstrual cycle. Written informed consent was obtained from all participants prior to enrollment in the study. The ethical review boards from the University of Manitoba, University of Nairobi, and Region Stockholm approved this study.

Measurements of progesterone and estradiol concentrations in the plasma were performed using the MILLIPLEX MAP Steroid/Thyroid Hormone Magnetic Bead Panel (Millipore, Merck, Darmstadt, Germany).

In Situ Fluorescence Staining and Image Analysis

A 3-mm^3 biopsy from the superior portion of the ectocervix was collected at 2 different time points and immediately snap-frozen in liquid nitrogen prior to storage at −80°C. Participants were examined by a gynecologist 3 days later to ensure proper healing. The women were counseled not to have sexual intercourse for 2 weeks after biopsy [20].

Immunofluorescence staining was performed on one 8-µm-thick section per staining from the cryopreserved tissue samples [18]. Among the study subjects, 15 cases and 22 controls were previously stained for expression of CD4, CCR5, and Langerin [18]. Four protocols were implemented to stain for CD4 together with E-cadherin, CCR5, Langerin, or CD3 using monoclonal primary antibodies followed by fluorochrome-conjugated secondary antibodies (Supplementary Table 1). Negative controls were incubated with secondary antibodies alone. All tissue sections were counterstained with 4',6-diamidino-2-phenylindole (DAPI) (Invitrogen, Thermo Fischer Scientific, Stockholm, Sweden) and scanned into digital images using a ×20 objective on a Pannoramic 250 Flash Slide Scanner (3DHistech Ltd, Budapest, Hungary). The epithelium was manually outlined as regions of interest (ROIs) prior to analysis. Two to six ROIs were outlined for each sample for quantitative image analysis, an average value per sample was used for statistics and graphs. Areas that exhibited broken tissue, cysts, or artifacts were excluded. Image analysis workflows using MatLab and CellProfiler [21] were developed and applied to assess grayscale images of each marker separately (CellProfiler workflow and instructions available at GitHub, https://github.com/gabriellaedf/Epithelial_Layers_and_Immune_Cells).

Epithelial Layer Segmentation

The net-like structure of E-cadherin was segmented using a contrast-independent approach [22] that accounts for varying intensity without creating erroneous breaks. Based on the E-cadherin net structure and nuclear staining, 4 epithelial layers were identified (Figure 1; Supplementary Figure 1). The superficial layer was defined as the area between a manually drawn line along the apical border of E-cadherin staining and the epithelial border (Figure 1A). The upper intermediate (IM) layer was represented by a disrupted E-cadherin net and the lower IM layer by an intact E-cadherin net (Figure 1B). To segment the 2 intermediate layers, all holes in the net structure were filled and spurs were removed, resulting in an object covering the intact E-cadherin net area. After masking out the parabasal layer, the remaining area was defined as the lower IM layer. The area between the lower IM layer and superficial layer was classified as the upper IM layer. The parabasal layer consists of 2–3 rows of highly packed cells that rest on the basal membrane. Nuclei located within approximately 2 µm of each other were merged, objects smaller than approximately 500 $µm^2$ were excluded, and the remaining objects were smoothed to represent the parabasal layer (Figure 1C).

Epithelial Integrity and Thickness Measurements

The segmented net-like structure of E-cadherin was used to assess epithelial integrity, namely the E-cadherin net coverage per area analyzed (%) and the mean fluorescence intensity (MFI). Another workflow was established to assess epithelial thickness. From the ROI outlines, an apical line following the epithelial apical border and a basal line following the basal membrane were segmented out. The distance from each point on the apical line to the nearest point on the basal line was calculated by creating a distance transform measuring the intensity (ie, distance) from the apical line to the corresponding basal line, and vice versa. The mean thickness of each of the 4 epithelial layers was calculated similarly.

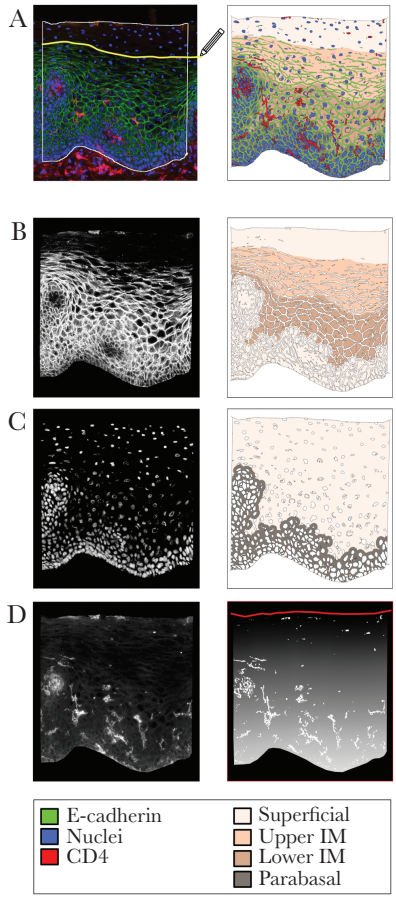

Figure 1. Schematic of the digital image analysis workflow developed for identifying mucosal markers of human immunodeficiency virus (HIV) susceptibility. Four distinct epithelial layers were objectively identified for subsequent analysis of markers of HIV susceptibility within each layer. *A*, Regions of interest within the ectocervical epithelium was manually outlined (white) in scanned images of immunostained, 2-dimensional tissue sections. The apical border of E-cadherin staining was manually outlined (yellow) to define the superficial layer (area above the line). Corresponding digital images (right column) show the 4 segmented epithelial layers, the integrity of the segmented E-cadherin net structure, and the spatial distribution of $CD4^+$ cells in the 4 layers. *B*, The intermediate layer (IM) was defined using the grayscale image of E-cadherin staining (left column), and divided into the upper IM layer represented by a nonintact or "leaky" E-cadherin net and the lower IM layer represented by an intact E-cadherin net (right column). *C*, The grayscale image of nuclei staining (left column) was used to identify the parabasal layer (dark brown, right column), based on the high nuclear density. *D*, The grayscale image of each immune cell marker (here CD4, left column) was used to segment out the positive stained area (white, right column) and measure the cell frequency per area analyzed. The spatial location of immune cells relative to the vaginal lumen was measured by overlaying the segmented $CD4^+$ cells (white, right column) with a distance transform (illustrated by a black-to-white gradient from the apical surface, marked in red, right column). In the distance transform image, all pixels were assigned a value representing the number of pixels (ie, distance) away from the apical line.

Segmentation of HIV Target Cells

Pixel-based segmentation, which has been reported to be appropriate for immune cells with irregular cell morphologies [23], was used to assess the CD4, CCR5, Langerin, and CD3 staining. A white top-hat noise-reduction filter was used in combination with automatically generated image-dependent intensity thresholds (Supplementary Table 2). The percentage of positively stained area within the total tissue area was used to represent the frequency of positive cells. Each marker was segmented individually and the overlapping area between co-stained markers was defined as double-positive.

Spatial Localization of Cellular Receptors

First, the average distance from the apical surface to the immune cells was assessed. A distance-transform image of the apical line was created, and the intensity/distance of the segmented cells was measured in this image (Figure 1D; Supplementary Figure 1C). Thereafter, the spatial distribution of cells across the 4 defined epithelial layers was measured. Using the thickness measurement of the layers as defined in the dual E-cadherin/CD4 staining, an approximate division of the superficial and upper IM layers was imposed on the CD4/CCR5-, CD4/Langerin-, and CD4/CD3-stained images. The proportion of the superficial and upper IM layers of the overall thickness was derived from E-cadherin staining and then applied to the total thickness calculation for each of the other stains. The parabasal layer was identified in each staining set. The lower IM layer was defined as the area between the parabasal layer and the approximated upper IM layer.

Statistical Methods

A Mann–Whitney *U* test was used to compare all continuous variables, and Pearson χ^2 test was applied for all categorical variables. Spearman correlation analysis was used to assess correlations between image data and hormone levels. Statistical analyses were performed using R software and $P < .05$ was considered statistically significant.

RESULTS

Study Participants and Sample Collection

Women from the Pumwani Sex Worker Cohort were recruited based on DMPA use (n = 30) or no hormonal contraceptive use (n = 40). No differences were observed in clinical and sociodemographic parameters between the groups (Table 1). All participants were sampled at 2 time points. The first sample was aimed for when the control subjects were in the luteal phase of the menstrual cycle, based on self-reported days since onset of last menses. Data were obtained from 35 of the 40 women (median, day 20 [range, 6–31]). The luteal phase, as defined by plasma progesterone levels >1.2 ng/mL [11], could be confirmed for all 35 participants. The second sample collected 2 weeks later (DMPA, n = 28 [overlapping subjects from first collection, n = 25]; controls, n = 32 [all overlapping]) aimed for the follicular phase for the controls. No differences were observed at this second time point between the study groups for the parameters listed in Table 1 (data not shown).

Table 1. Clinical Characteristics of Study Subjects

Characteristic	DMPA (n = 30)	Controls Luteal Phase (n = 40)	*P* Value
Age, y, median (range)	30 (22–41)	31 (20–47)	.961[a]
Not available, No.	0	1	
Months in sex work, median (range)	24 (3–36)	24 (4–36)	.203[a]
Not available, No.	0	2	
No. of clients last 7 d, median (range)	5 (0–28)	4 (0–30)	.757[a]
Not available, No.	4	2	
Condom use last 7 d, median (range)	100% (50–100)	100% (67–100)	.919[a]
Not available, No.	5	5	
Having a regular partner, No. (%)			.458[b]
Yes	16 (53%)	24 (60%)	
No	11 (37%)	15 (37%)	
Not available	3 (10%)	1 (3%)	
Practice vaginal douching, No. (%)			.125[b]
Yes	11 (37%)	9 (22%)	
No	16 (53%)	30 (75%)	
Not available	3 (10%)	1 (3%)	
Bacterial vaginosis (Nugent score), No. (%)			.623[b]
Normal (0–3)	17 (57%)	23 (58%)	
Intermediate (4–6)	7 (23%)	7 (18%)	
BV (7–10)	4 (13%)	9 (22%)	
Not available	2 (7%)	1 (2%)	
Genital infection[c], No. (%)			.362[b]
Chlamydia trachomatis	0 (0%)	1 (2%)	
Neisseria gonorroheae	1 (3%)	1 (2%)	

Abbreviations: BV, bacterial vaginosis; DMPA, depot medroxyprogesterone acetate.

[a]Mann–Whitney *U* test.

[b]Pearson χ^2 test.

[c]Screening for genital infection was negative at baseline (inclusion criteria).

DMPA Users Exhibit a Thinner Superficial Layer in the Ectocervix

Image analysis workflows were established to differentiate the epithelium into 4 layers and to quantify the E-cadherin net coverage (%) and MFI. Comparable epithelial tissue areas were analyzed in both study groups for all staining (Supplementary Table 3); for each subject a total of approximately 2400 cells were analyzed per staining. All measurements were normalized against the total tissue area analyzed. E-cadherin net coverage was absent from the superficial layer but present in high abundance in the other layers (Figures 1A, 1B and 2A). Compared to controls in the luteal phase, DMPA users showed similar levels of E-cadherin net coverage (29%), but lower compared with controls in the follicular phase (29% vs 33%, $P = .001$) (data not shown). This difference was specific to the lower IM (32% vs 37%, $P = .0001$) and parabasal layers (33% vs 39%, $P = .009$) (Figure 2B). The MFI of E-cadherin expression was comparable in all layers between the study groups (Supplementary Figure 2).

Next, we designed a workflow to measure the thickness of each epithelial layer, taking into account that the epithelium is irregular with a sinuous-patterned basal membrane and a relatively straight apical surface. Although the total thickness was comparable between DMPA users and controls, the DMPA group displayed a thinner superficial layer compared to controls in both the luteal phase (23 vs 46 μm, $P = .002$) and follicular phase (36 vs 65 μm, $P = .0007$) (Figure 2C and 2D). Moreover, compared to controls in the follicular phase, DMPA users displayed a thicker upper IM layer (corresponding to a larger area of disrupted E-cadherin net structure) (86 vs 72 μm, $P = .03$), whereas the lower IM and parabasal layers exhibited similar thicknesses (Figure 2D).

Mucosal CD4$^+$ Cells Are More Superficially Located in DMPA Users

We developed a workflow to examine the quantity and spatial distribution of CD4$^+$ cells within ectocervical epithelium to understand the effect of DMPA on immune cell frequency/localization. First, single CD4$^+$ cells were assessed in conjunction with E-cadherin staining (Figure 2A), and no differences in the frequency of CD4$^+$ cells were observed between DMPA users and controls (Figure 3A). These CD4$^+$ cells were located closer to the apical surface in the DMPA group vs luteal phase controls (194 vs 220 μm, $P = .04$), but equal to follicular phase controls (Figure 3B). Women using DMPA also had a higher proportion of CD4$^+$ cells in the upper IM layer compared with control women in either menstrual phase (luteal phase: 17% vs 7%, $P = .0009$; follicular phase: 18% vs 10%, $P = .002$), as well as a lower proportion of CD4$^+$ cells in the lower IM layer (luteal phase: 41 % vs 48%, $P = .03$; follicular phase: 34% vs 45%,

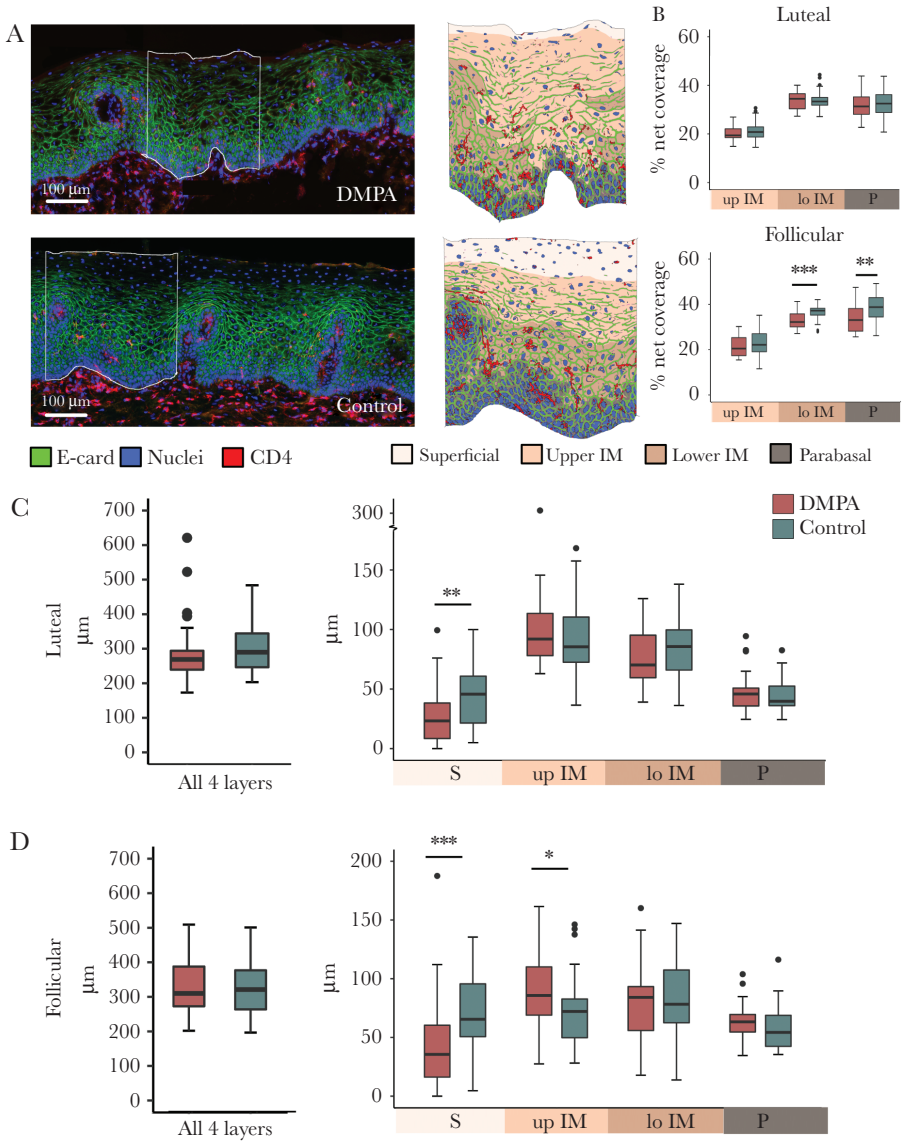

Figure 2. Epithelial integrity and thickness of the ectocervical epithelium. *A*, Representative image of immunostaining (left) and identified layers (right) of an ectocervical tissue section obtained from a depot medroxyprogesterone acetate (DMPA) user and control subject (no hormonal contraceptive use) stained for E-cadherin and CD4. *B*, Boxplots showing E-cadherin net coverage (ie, the percentage of E-cadherin net structure area out of area analyzed) in the 3 epithelial layers. Comparison of DMPA users vs control subjects in the luteal (top) and follicular (bottom) phases. Boxplots showing total epithelial thickness, as well as the thickness of the 4 individual layers in DMPA users vs control subjects in the luteal phase (*C*) and in the follicular phase (*D*). Boxplot: median (interquartile range [IQR]); error bars: largest/smallest value within 1.5 × IQR; outside values marked as dots. **P* < .05, ***P* < .01, ****P* < .001. Each datapoint represents 1 subject. Abbreviations: lo IM, lower intermediate; P, parabasal; S, superficial; up IM, upper intermediate.

P = .02) (Figure 3C). Both groups exhibited an equal proportion of $CD4^+$ cells in the parabasal layer (Figure 3C) and none in the superficial layer (data not shown).

HIV Target Cells Are Distributed More Apically in the Ectocervix of DMPA Users

Next, we investigated CD4 staining in combination with CCR5, Langerin, or CD3 staining as HIV target cells express these cell-surface markers. DMPA samples were compared against control samples collected during the luteal phase for these analyses. The frequency of total $CD4^+CCR5^+$ cells (Figure 4A) was similar between the groups (Figure 5A). However, within the total $CD4^+$ cell population, the proportion of $CD4^+CCR5^+$ cells was higher in the DMPA group (38% vs 24%, *P* = .007) (Figure 5B). While $CD4^+CCR5^+$ cells were located at a median distance of 217 µm from the apical surface in both groups (Figure 5C), the DMPA group exhibited a higher proportion of $CD4^+CCR5^+$ cells in the upper IM layer (10% vs 5%, *P* = .009) (Figure 5D) but a lower proportion in the parabasal layer (57% vs 63%, *P* = .04) (Figure 5D). The majority of $CD4^+CCR5^+$ cells were found in the parabasal layer

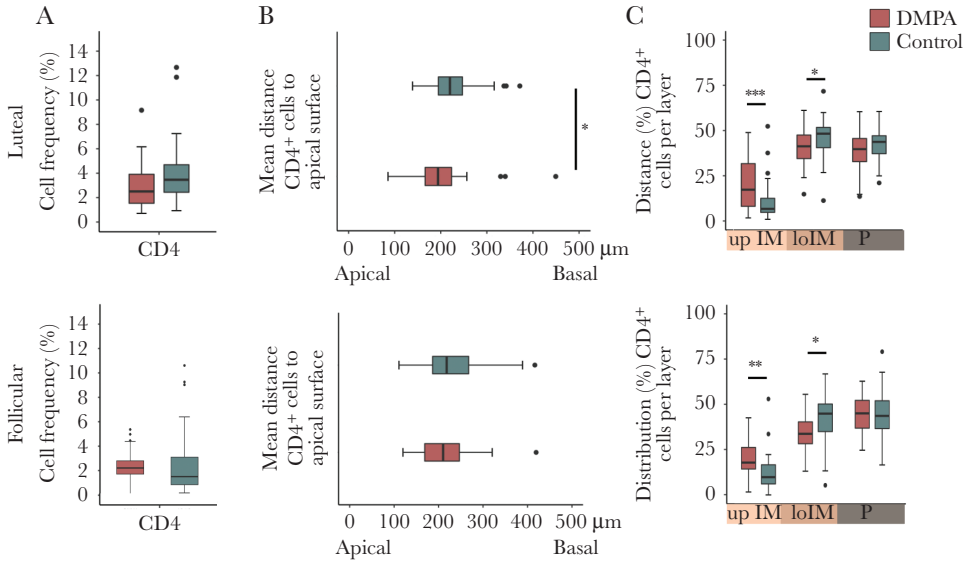

Figure 3. Expression and spatial localization of CD4$^+$ cells. Graphs showing the comparisons between depot medroxyprogesterone acetate users vs control subjects in the luteal (top) and follicular (bottom) phases. *A*, The frequency of CD4$^+$ cells in the ectocervical epithelium (defined as CD4 positive area/area analyzed). *B*, The mean distance from the epithelial surface to CD4$^+$ cells. *C*, Distribution of CD4$^+$ cells located in each of the 3 epithelial layers. Boxplot: median (interquartile range [IQR]); error bars: largest/smallest value within 1.5 × IQR; outside values marked as dots. *P < .05; **P < .01. Each datapoint represents 1 subject. Abbreviations: DMPA, depot medroxyprogesterone acetate; lo IM, lower intermediate; P, parabasal; up IM, upper intermediate.

in both groups (Figure 5D). The CCR5$^+$ staining was similar to CD4$^+$CCR5$^+$ staining (Supplementary Figure 3).

Quantification of CD4 and Langerin staining (Figure 4B) showed that the DMPA group had a lower frequency of CD4$^+$Langerin$^+$ cells (0.4% vs 0.6%, P = .03) (Figure 5A). The proportion of CD4$^+$Langerin$^+$ cells among the total CD4$^+$ cell population was also lower for the DMPA group (19% vs 25%, P = .008) (Figure 5B). CD4$^+$Langerin$^+$ cells were localized more superficially in DMPA users (172 vs 216 µm, P = .008) (Figure 5C), and they also displayed a higher proportion of CD4$^+$Langerin$^+$ cells in the upper IM layer compared with the control group (15% vs 9%, P = .003) (Figure 5D). In both groups, the majority of CD4$^+$Langerin$^+$ cells were found in the lower IM layer, followed by the parabasal layer (Figure 5D). The Langerin$^+$ staining was similar to CD4$^+$Langerin$^+$ staining (Supplementary Figure 3).

Next, we investigated the frequency and localization of CD4$^+$CD3$^+$ cells in a subset of samples (DMPA, n = 16; controls, n = 35) (Figure 4C). Both groups were comparable for the parameters listed in Table 1 (data not shown). No differences were seen in the frequency of CD4$^+$CD3$^+$ cells (Figure 5A). However, the DMPA group displayed a higher proportion of CD4$^+$CD3$^+$ cells among the total CD4$^+$ cell population compared with the control group (19% vs 14%, P = .007) (Figure 5B). Although CD4$^+$CD3$^+$ cells were located at a similar distance from the epithelial apical surface in both groups (Figure 5C), DMPA users had a higher proportion of these cells in the upper IM layer (9% vs 6%, P = .02) (Figure 5D), with the majority of the CD4$^+$CD3$^+$ cells found in the parabasal layer (Figure 5D). The CD3$^+$ staining was similar to that of CD4$^+$CD3$^+$ staining (Supplementary Figure 3).

Systemic Estradiol Levels Affect E-Cadherin Expression and Localization of CD4$^+$CCR5$^+$ and CD4$^+$Langerin$^+$ Cells

Assessment of plasma hormone levels within the control group, at the luteal phase, revealed a positive correlation between estradiol and the MFI of E-cadherin staining in the upper IM (P = .02, r = 0.40), lower IM (P = .03, r = 0.37), and parabasal layers (P = .03, r = 0.37) (Figure 6A). A negative correlation was observed between estradiol and parabasal thickness (P = .04, r = −0.36) (Figure 6B). A negative correlation was also seen between estradiol and the proportion of CD4$^+$CCR5$^+$ cells located in the lower IM layer (P = .01, r = −0.43), while a positive correlation was found in the proportion of CD4$^+$CCR5$^+$ cells localized in the parabasal layer (P = .009, r = 0.44) (Figure 6C). In addition, a negative correlation with estradiol was seen with the proportion of CD4$^+$Langerin$^+$ cells located in the lower IM layer (P = .05, r = −0.34) (Figure 6D). No other correlations were observed for the remaining measurements (Figure 5), nor for progesterone relative to any tissue parameter (Supplementary Figure 4).

DISCUSSION

We here revealed that Kenyan sex workers who regularly use DMPA displayed a less intact ectocervical epithelium with more superficially located HIV target cells compared to women not using hormonal contraceptives. This mucosal signature can have the capacity to affect an individual's HIV susceptibility risk.

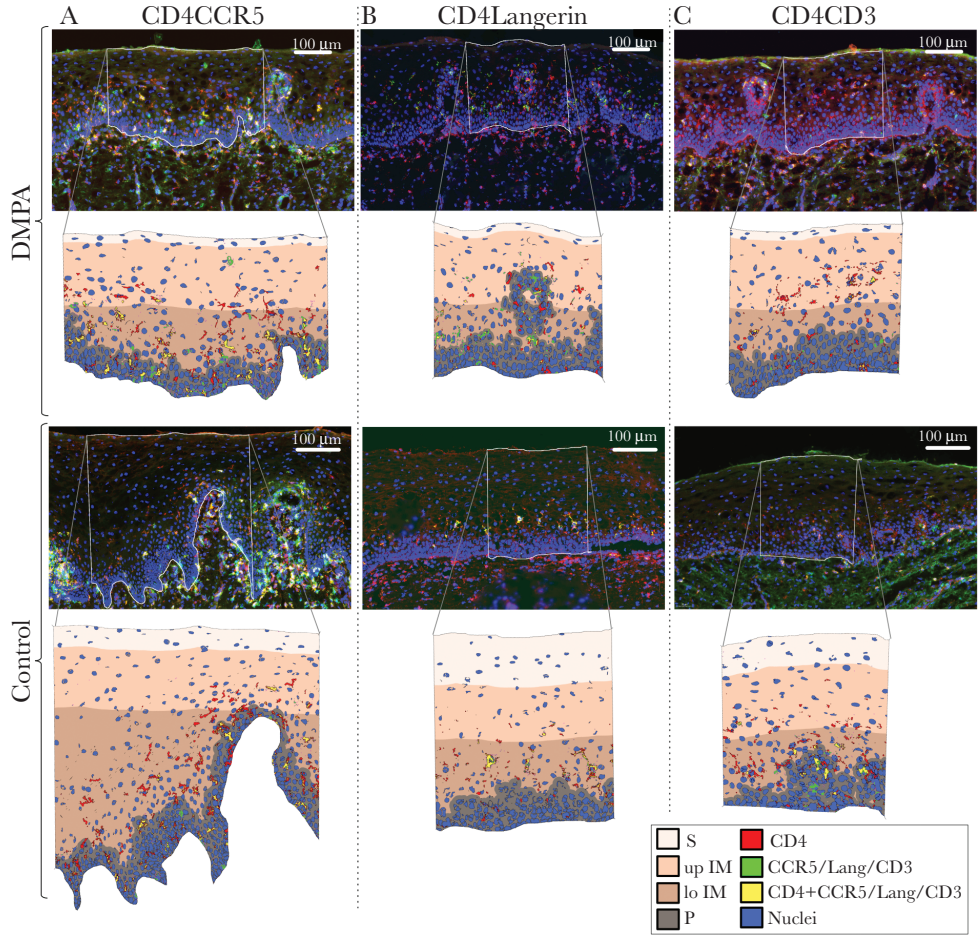

Figure 4. Human immunodeficiency virus target cells visualized by immunostaining. Representative images of immunostained ectocervical tissue and enlarged regions of interest that show digital representations of the spatial localization of double-stained cells in each of the 4 identified epithelial layers in depot medroxyprogesterone acetate users (top) and control subjects in the luteal phase (bottom). *A*, CD4 and CCR5 staining. *B*, CD4 and Langerin staining. *C*, CD4 and CD3 staining. Abbreviations: DMPA, depot medroxyprogesterone acetate; lo IM, lower intermediate; P, parabasal; S, superficial; up IM, upper intermediate.

The active progestin compound of DMPA, medroxyprogesterone acetate (MPA), suppresses estradiol and progesterone levels [24]. To better understand how DMPA usage affects the genital mucosa, we therefore sampled the control group during both their luteal and follicular menstrual phases to account for natural sex hormone variations. Likewise, to aim for comparable MPA concentrations among the DMPA users [24], the women were targeted for inclusion within a 2- to 6-week period since their last injection, and for being on treatment for at least 6 months. Interestingly, a recent report correlated MPA concentration with reduced cervicovaginal growth factor expression in human mucosa [25]. However, because we lacked the capability to directly measure the plasma MPA concentration, it was not possible to correlate MPA levels to the mucosal study parameters. Our novel image-based workflows revealed that DMPA users possess a thinner superficial epithelium and showed more apical distribution of $CD4^+$ cells compared to both follicular and luteal samples from the control group. The E-cadherin net coverage was comparable between DMPA users and control women in the luteal phase, but was lower than the control women in the follicular phase. These data imply that endogenous estradiol levels may influence E-cadherin expression, which was supported by a correlation found between plasma estradiol levels and intensity of E-cadherin expression in all epithelial layers. Estradiol levels were also positively correlated to E-cadherin net coverage in the upper IM layer. With $r < 0.5$, these correlations were weak but indicate an association between plasma levels and tissue parameters, as local hormone concentration in tissue was not available. Sex hormones can influence epithelial junction protein expression directly through transcriptional regulation [9, 17] or through effects on the genital microflora and protein expression [10, 26, 27]. Here, we could not discern whether the effects on E-cadherin were caused by DMPA, the hypoestrogenic/hypoprogestogenic state, or other factors. However, it is likely that DMPA use led to the thinning of the superficial epithelial lining and apical distribution of $CD4^+$ cells, as these outcomes were not observed in any of

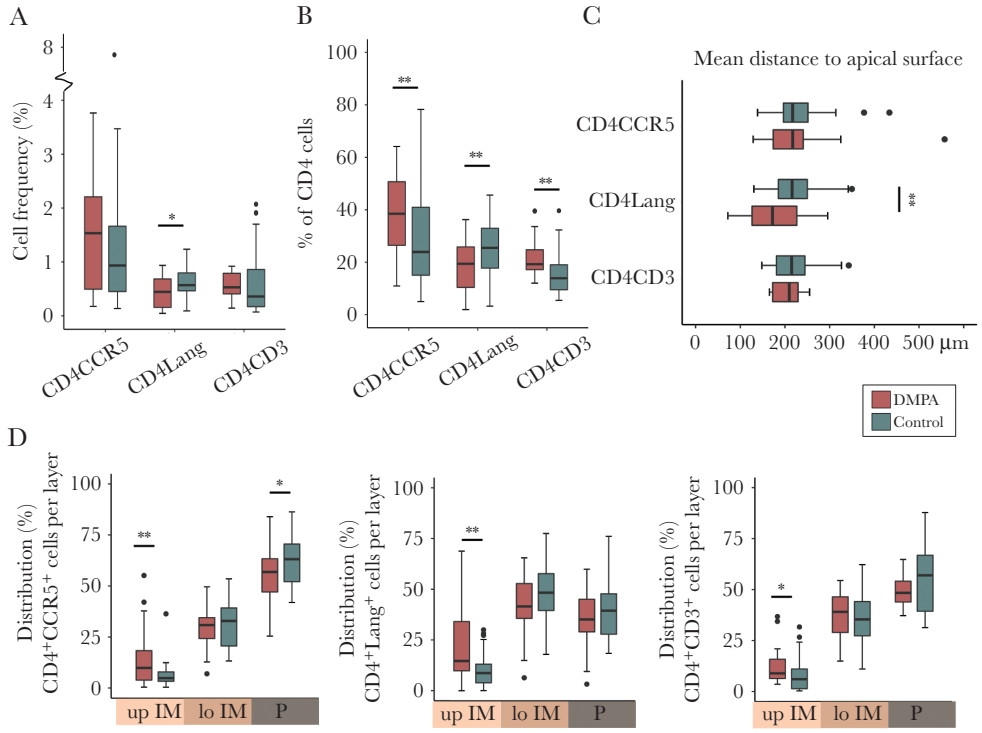

Figure 5. Quantification and spatial localization of human immunodeficiency virus (HIV) target cells. *A*, Quantification of cell frequencies identified by double-staining of HIV target cells in the ectocervical epithelium in depot medroxyprogesterone acetate (DMPA) users and control subjects in the luteal phase (frequency defined as positive area/area analyzed) *B*, Proportion of $CD4^+$ cells that co-express CCR5, Langerin, or CD3 in DMPA users and control subjects in the luteal phase. *C*, Mean distance between the epithelial surface and the HIV target cells for DMPA users and control subjects in the luteal phase. *D*, Graphs showing the distribution of cells located in each of the 3 epithelial layers: $CD4^+CCR5^+$ (left), $CD4^+Langerin^+$ (middle), and $CD4^+CD3^+$ (right) cells. Boxplot: median (interquartile range [IQR]); error bars: largest/smallest value within 1.5 × IQR; outside values marked as dots. $^*P < .05$; $^{**}P < .01$. Each datapoint represents 1 subject. Abbreviations: DMPA, depot medroxyprogesterone acetate; lo IM, lower intermediate; P, parabasal; up IM, upper intermediate.

the control groups. Moreover, these parameters lacked a correlation with progesterone and estradiol levels.

The thinner superficial epithelial layer seen in DMPA users can be a contributing factor for viral entry, as suggested in both experimental and clinical studies [10, 12, 17, 28, 29]. HIV particles can passively penetrate epithelial layers lacking cell junctions to areas where target cells are located [30]. As the vaginal and ectocervical epithelium are structurally similar, our present study is comparable to studies on the vaginal epithelium showing that neither progestin-based hormonal contraceptive users, nor women during the luteal phase, displayed significant changes in total epithelial thickness [12, 27, 31–35]. This current study, as well as our previous one that focused on users of progesterone-based intrauterine devices [36], demonstrates the need to explore individual epithelial segments to reveal functional differences.

To explore the localization of HIV target cells during DMPA usage, we established a new workflow based on our previous knowledge assessing immune cells in tissue [18, 37–39]. The frequency of $CD4^+CCR5^+$ and $CD4^+CD3^+$ cells within the total $CD4^+$ population in the epithelium, as well as the distribution of these cells in the upper IM layer, was higher in DMPA users than in the luteal phase control group. Although the DMPA group showed a lower frequency of total $CD4^+Langerin^+$ cells, these cells were more abundant in the upper IM layer and located closer to the apical surface. The upper IM layer was here characterized by a disrupted E-cadherin net, suggesting that cells present in this tissue location are more accessible for HIV. HIV proteins can interact with epithelial cells to disrupt epithelial junction proteins, which results in reduced barrier functions that facilitates spread of viruses [40, 41]. A more apical distribution of T cells and $Langerin^+$ cells in the vaginal epithelium has been reported previously in DMPA users [16]. DMPA has been associated with increased expression of genital inflammatory proteins, number of activated T cells, and epithelial disruption [10, 11, 13, 18, 42–44], all of which could explain why mucosal HIV target cells are recruited to the apical surface. The DMPA-induced hypoestrogenic/hypoprogestogenic state could also contribute to this apical localization since we show here that higher estradiol levels correlated with a basal location of $CD4^+CCR5^+$ cells. Increased immune cell density in vaginal tissue samples of women using DMPA has been recorded in some [12, 45], but not all [16, 32, 46] studies. HIV target cell numbers were also increased in the endocervical mucosa of DMPA-treated non-human primates [47].

The novel quantitative image analysis approach presented here capitalizes on emerging developments in

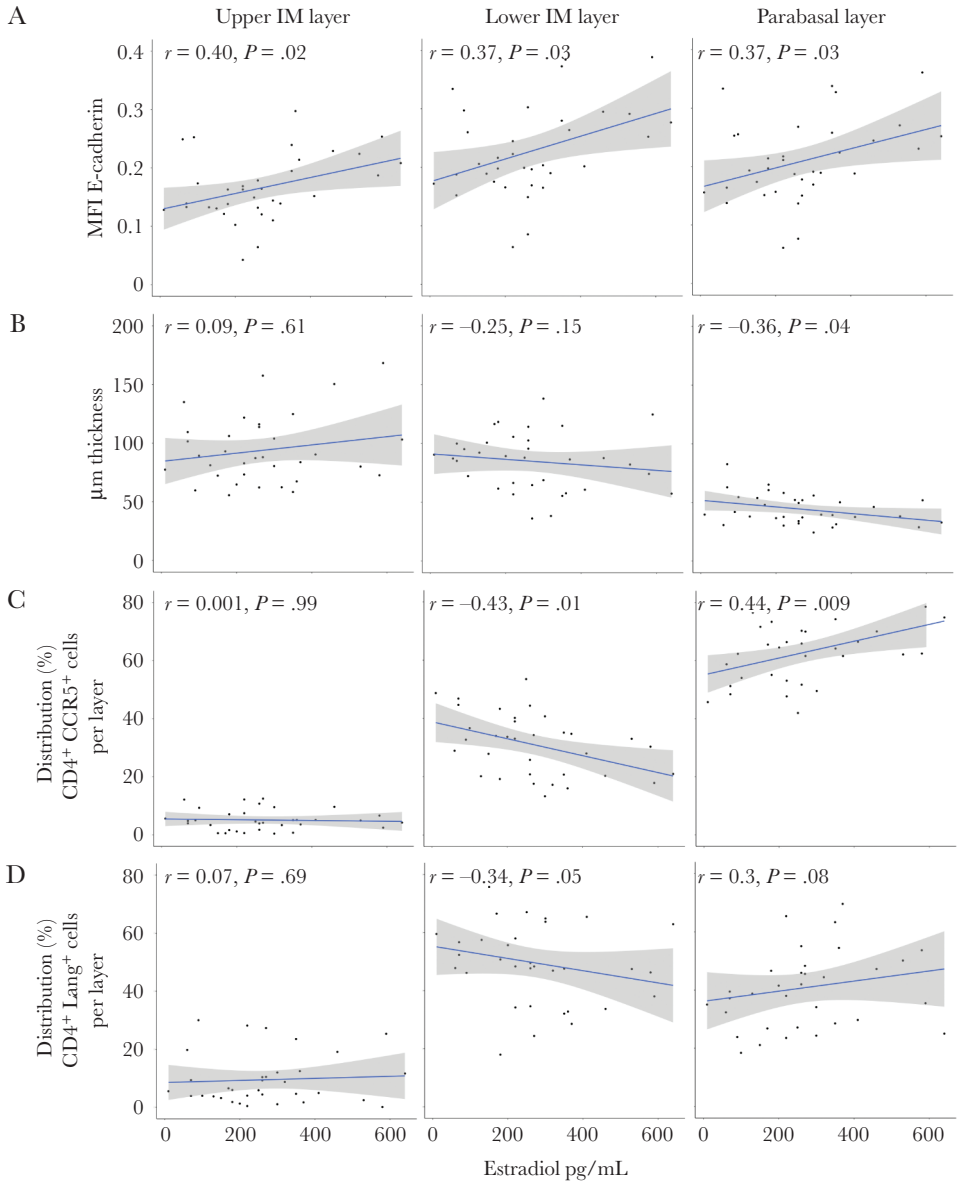

Figure 6. Correlations to systemic estradiol levels. Correlations between systemic estradiol levels in control subjects in the luteal phase and mean fluorescence intesity (MFI) of E-cadherin (*A*), epithelial thickness (*B*), distribution of $CD4^+CCR5^+$ cells (*C*), and distribution of $CD4^+Langerin^+$ cells (*D*) in the ectocervical epithelial upper intermediate (IM) layer (left), lower IM layer (middle), and parabasal layer (right). Graphs show Spearman correlation with a linear regression line and 95% confidence interval (gray). Each datapoint represents 1 subject.

high-throughput processing of digital image data from tissue slides to enable standardized objective measurements. Our novel assay assessed approximately 2500 cells over a 600-μm^2 surface area per subject. All measurements were performed on thin 2-dimensional sections that were assumed to represent the local 3-dimensional structure of the tissue samples. However, potential limitations exist, including intersubject variation in staining intensity and the natural variability of tissue morphology. Our image analysis workflows overcame these challenges with robust algorithms and read-out set points. These workflows can therefore be adapted for studies on other epithelial linings and their associated immune cells, such as evaluations of experimental antiviral or vaccine compounds on mucosal surfaces or investigations into contraceptives that lack association with HIV susceptibility to influence clinical guidelines for their use.

Supplementary Data

Supplementary materials are available at *The Journal of Infectious Diseases* online. Consisting of data provided by the authors to benefit the reader, the posted materials are not copyedited and are the sole responsibility of the authors, so questions or comments should be addressed to the corresponding author.

Notes

Acknowledgments. The authors thank the research participants and the Majengo clinic staff for their support and time; Dr Angela Muliro for performing the examinations and biopsies; Julianna Cheruiyot for coordinating the research participants; Geneviève Boily-Larouche for help in coordinating the early stage of the study; and Fariba Foroogh for technical assistance.

Financial support. This work was supported by the Karolinska Institutet faculty funds for the graduate program in international ranking (to G. E., K. B., and A.T.); the Erik and Edit Färnström Foundation (to G. E.); the Swedish Physicians Against AIDS Foundation (to M. R.); the European Research Council (https://erc.europa.eu/funding/consolidator-grants, reference number 682810 to C. W.); the Canadian Institutes of Health Research (https://cihr-irsc.gc.ca/e/193.html, reference number 86721 to K. R. F.); and the Swedish Research Council (http://www.vr.se, reference number 201605762 to K. B.).

Potential conflicts of interest. All authors: No reported conflicts of interest.

All authors have submitted the ICMJE Form for Disclosure of Potential Conflicts of Interest. Conflicts that the editors consider relevant to the content of the manuscript have been disclosed.

References

1. Joint United Nations Programme on HIV/AIDS. UNAIDS data 2019. Geneva, Switzerland: UNAIDS, **2019**.
2. United Nations. Contraceptive use by method 2019. Available at: https://www.un.org/development/desa/pd/sites/www.un.org.development.desa.pd/files/files/documents/2020/Jan/un_2019_contraceptiveusebymethod_databooklet.pdf. Accessed 21 August 2020.
3. Morrison CS, Chen PL, Kwok C, et al. Hormonal contraception and the risk of HIV acquisition: an individual participant data meta-analysis. PLoS Med **2015**; 12:e1001778.
4. Polis CB, Curtis KM, Hannaford PC, et al. An updated systematic review of epidemiological evidence on hormonal contraceptive methods and HIV acquisition in women. AIDS **2016**; 30:2665–83.
5. Ralph LJ, McCoy SI, Shiu K, Padian NS. Hormonal contraceptive use and women's risk of HIV acquisition: a meta-analysis of observational studies. Lancet Infect Dis **2015**; 15:181–9.
6. Evidence for Contraceptive Options and HIV Outcomes (ECHO) Trial Consortium. HIV incidence among women using intramuscular depot medroxyprogesterone acetate, a copper intrauterine device, or a levonorgestrel implant for contraception: a randomised, multicentre, open-label trial. Lancet **2019**; 394:303–13.
7. Hapgood JP. Is the injectable contraceptive depo-medroxyprogesterone acetate (DMPA-IM) associated with an increased risk for HIV acquisition? The jury is still out. AIDS Res Hum Retroviruses **2019**; 36:357–66.
8. Sathyamala C. Depot contraception and HIV: an exercise in obfuscation. BMJ **2019**; 367:l5768.
9. Hapgood JP, Kaushic C, Hel Z. Hormonal contraception and HIV-1 acquisition: biological mechanisms. Endocr Rev **2018**; 39:36–78.
10. Birse KD, Romas LM, Guthrie BL, et al. Genital injury signatures and microbiome alterations associated with depot medroxyprogesterone acetate usage and intravaginal drying practices. J Infect Dis **2017**; 215:590–8.
11. Byrne EH, Anahtar MN, Cohen KE, et al. Association between injectable progestin-only contraceptives and HIV acquisition and HIV target cell frequency in the female genital tract in South African women: a prospective cohort study. Lancet Infect Dis **2016**; 16:441–8.
12. Chandra N, Thurman AR, Anderson S, et al. Depot medroxyprogesterone acetate increases immune cell numbers and activation markers in human vaginal mucosal tissues. AIDS Res Hum Retroviruses **2013**; 29:592–601.
13. Deese J, Masson L, Miller W, et al. Injectable progestin-only contraception is associated with increased levels of pro-inflammatory cytokines in the female genital tract. Am J Reprod Immunol **2015**; 74:357–67.
14. Guthrie BL, Introini A, Roxby AC, et al. Depot medroxyprogesterone acetate use is associated with elevated innate immune effector molecules in cervicovaginal secretions of HIV-1-uninfected women. J Acquir Immune Defic Syndr **2015**; 69:1–10.
15. Huijbregts RP, Michel KG, Hel Z. Effect of progestins on immunity: medroxyprogesterone but not norethisterone or levonorgestrel suppresses the function of T cells and pDCs. Contraception **2014**; 90:123–9.
16. Michel KG, Huijbregts RP, Gleason JL, Richter HE, Hel Z. Effect of hormonal contraception on the function of plasmacytoid dendritic cells and distribution of immune cell populations in the female reproductive tract. J Acquir Immune Defic Syndr **2015**; 68:511–8.
17. Zalenskaya IA, Chandra N, Yousefieh N, et al. Use of contraceptive depot medroxyprogesterone acetate is associated with impaired cervicovaginal mucosal integrity. J Clin Invest **2018**; 128:4622–38.
18. Lajoie J, Tjernlund A, Omollo K, et al. Increased cervical CD4(+)CCR5(+) T cells among Kenyan sex working women using depot medroxyprogesterone acetate. AIDS Res Hum Retroviruses **2019**; 35:236–46.
19. Boily-Larouche G, Lajoie J, Dufault B, et al. Characterization of the genital mucosa immune profile to distinguish phases of the menstrual cycle: implications for HIV susceptibility. J Infect Dis **2019**; 219:856–66.

20. Lajoie J, Boily-Larouche G, Doering K, et al. Improving adherence to post-cervical biopsy sexual abstinence in Kenyan female sex workers. Am J Reprod Immunol **2016**; 76:82–93.
21. McQuin C, Goodman A, Chernyshev V, et al. CellProfiler 3.0: next-generation image processing for biology. PLoS Biol **2018**; 16:e2005970.
22. Obara B, Fricker M, Gavaghan D, Grau V. Contrast-independent curvilinear structure detection in biomedical images. IEEE Trans Image Process **2012**; 21:2572–81.
23. Saylor J, Ma Z, Goodridge HS, et al. Spatial mapping of myeloid cells and macrophages by multiplexed tissue staining. Front Immunol **2018**; 9:2925.
24. Mishell DR Jr. Pharmacokinetics of depot medroxyprogesterone acetate contraception. J Reprod Med **1996**; 41:381–90.
25. Molatlhegi RP, Liebenberg LJ, Leslie A, et al. Plasma concentration of injectable contraceptive correlates with reduced cervicovaginal growth factor expression in South African women. Mucosal Immunol **2020**; 13:449–59.
26. Jespers V, Kyongo J, Joseph S, et al. A longitudinal analysis of the vaginal microbiota and vaginal immune mediators in women from sub-Saharan Africa. Sci Rep **2017**; 7:11974.
27. Miller L, Patton DL, Meier A, Thwin SS, Hooton TM, Eschenbach DA. Depomedroxyprogesterone-induced hypoestrogenism and changes in vaginal flora and epithelium. Obstet Gynecol **2000**; 96:431–9.
28. Ferreira VH, Dizzell S, Nazli A, et al. Medroxyprogesterone acetate regulates HIV-1 uptake and transcytosis but not replication in primary genital epithelial cells, resulting in enhanced T-cell infection. J Infect Dis **2015**; 211:1745–56.
29. Quispe Calla NE, Vicetti Miguel RD, Boyaka PN, et al. Medroxyprogesterone acetate and levonorgestrel increase genital mucosal permeability and enhance susceptibility to genital herpes simplex virus type 2 infection. Mucosal Immunol **2016**; 9:1571–83.
30. Carias AM, McCoombe S, McRaven M, et al. Defining the interaction of HIV-1 with the mucosal barriers of the female reproductive tract. J Virol **2013**; 87:11388–400.
31. Bahamondes L, Trevisan M, Andrade L, et al. The effect upon the human vaginal histology of the long-term use of the injectable contraceptive Depo-Provera. Contraception **2000**; 62:23–7.
32. Bahamondes MV, Castro S, Marchi NM, et al. Human vaginal histology in long-term users of the injectable contraceptive depot-medroxyprogesterone acetate. Contraception **2014**; 90:117–22.
33. Eschenbach DA, Patton DL, Meier A, et al. Effects of oral contraceptive pill use on vaginal flora and vaginal epithelium. Contraception **2000**; 62:107–12.
34. Mauck CK, Callahan MM, Baker J, et al. The effect of one injection of Depo-Provera on the human vaginal epithelium and cervical ectopy. Contraception **1999**; 60:15–24.
35. Patton DL, Thwin SS, Meier A, Hooton TM, Stapleton AE, Eschenbach DA. Epithelial cell layer thickness and immune cell populations in the normal human vagina at different stages of the menstrual cycle. Am J Obstet Gynecol **2000**; 183:967–73.
36. Tjernlund A, Carias AM, Andersson S, et al. Progesterone-based intrauterine device use is associated with a thinner apical layer of the human ectocervical epithelium and a lower ZO-1 mRNA expression. Biol Reprod **2015**; 92:68.
37. Gibbs A, Buggert M, Edfeldt G, et al. Human immunodeficiency virus-infected women have high numbers of CD103-CD8+ T cells residing close to the basal membrane of the ectocervical epithelium. J Infect Dis **2018**; 218:453–65.
38. Gibbs A, Leeansyah E, Introini A, et al. MAIT cells reside in the female genital mucosa and are biased towards IL-17 and IL-22 production in response to bacterial stimulation. Mucosal Immunol **2017**; 10:35–45.
39. Gunaydin G, Edfeldt G, Garber DA, et al. Impact of Q-Griffithsin anti-HIV microbicide gel in non-human primates: in situ analyses of epithelial and immune cell markers in rectal mucosa. Sci Rep **2019**; 9:18120.
40. Lien K, Mayer W, Herrera R, Rosbe K, Tugizov SM. HIV-1 proteins gp120 and tat induce the epithelial-mesenchymal transition in oral and genital mucosal epithelial cells. PLoS One **2019**; 14:e0226343.
41. Tugizov S. Human immunodeficiency virus-associated disruption of mucosal barriers and its role in HIV transmission and pathogenesis of HIV/AIDS disease. Tissue Barriers **2016**; 4:e1159276.
42. Fichorova RN, Chen PL, Morrison CS, et al. The contribution of cervicovaginal infections to the immunomodulatory effects of hormonal contraception. mBio **2015**; 6:e00221-15.
43. Goldfien GA, Barragan F, Chen J, et al. Progestin-containing contraceptives alter expression of host defense-related genes of the endometrium and cervix. Reprod Sci **2015**; 22:814–28.
44. Li L, Zhou J, Wang W, et al. Effects of three long-acting reversible contraceptive methods on HIV target cells in the human uterine cervix and peripheral blood. Reprod Biol Endocrinol **2019**; 17:26.
45. Thurman A, Chandra N, Schwartz JL, et al. The effect of hormonal contraception on cervicovaginal mucosal end points associated with HIV acquisition. AIDS Res Hum Retroviruses **2019**; 35:853–64.
46. Mitchell CM, McLemore L, Westerberg K, et al. Long-term effect of depot medroxyprogesterone acetate on vaginal microbiota, epithelial thickness and HIV target cells. J Infect Dis **2014**; 210:651–5.
47. Goode D, Aravantinou M, Jarl S, et al. Sex hormones selectively impact the endocervical mucosal microenvironment: implications for HIV transmission. PLoS One **2014**; 9:e97767.